VIRUS: a massively replicated 33k fiber integral field spectrograph for the upgraded Hobby-Eberly Telescope[*]

Gary. J. Hill[a†], Hanshin Lee[a], Brian L. Vattiat[a], Joshua J. Adams[b], J.L. Marshall[c], Niv Drory[d], D.L. DePoy[c], Guillermo Blanc[b], Ralf Bender[d,e], John A. Booth[a], Taylor Chonis[a], Mark E. Cornell[a], Karl Gebhardt[b], John Good[a], Frank Grupp[e], Roger Haynes[f,g], Andreas Kelz[f], Phillip J. MacQueen[a], Nick Mollison[h], J. D. Murphy[b], M.D. Rafal[a], W. N. Rambold[f,g], M.M. Roth[f,g], R. Savage[a], & M.P. Smith[i]

[a] McDonald Observatory, [b]Department of Astronomy, University of Texas at Austin, 1 University Station, Austin, TX 78712-0259, USA

[c] Department of Physics and Astronomy, Texas A&M University, 4242 TAMU, College Station, TX 77843-4242, USA

[d] Max-Planck-Institut für Extraterrestriche-Physik, Giessenbachstrasse, D-85748 Garching b. München, Germany

[e] Universitäts-Sternwarte München, Scheinerstr. 1 , 81679 München, Germany

[f] Astrophysikalisches Institut Potsdam, An der Sternwarte 16, 14482 Potsdam, Germany

[g]innoFSPEC Potsdam, An der Sternwarte 16, 14482 Potsdam, Germany

[h] Center for Electromechanics, University of Texas at Austin, 1 University Station R7000, Austin, TX 78712, USA

[i] Department of Astronomy, University of Wisconsin-Madison, 3321 Sterling Hall, 475 N. Charter Street, Madison WI 53706-1582, USA

ABSTRACT

The Visible Integral-field Replicable Unit Spectrograph (VIRUS) consists of a baseline build of 150 identical spectrographs (arrayed as 75 units, each with a pair of spectrographs) fed by 33,600 fibers, each 1.5 arcsec diameter, deployed over the 22 arcminute field of the upgraded 10 m Hobby-Eberly Telescope (HET). The goal is to deploy 96 units. VIRUS has a fixed bandpass of 350-550 nm and resolving power R~700. VIRUS is the first example of industrial-scale replication applied to optical astronomy and is capable of spectral surveys of large areas of sky. The method of industrial replication, in which a relatively simple, inexpensive, unit spectrograph is copied in large numbers, offers significant savings of engineering effort, cost, and schedule when compared to traditional instruments.

The main motivator for VIRUS is to map the evolution of dark energy for the Hobby-Eberly Telescope Dark Energy Experiment (HETDEX[‡]) using 0.8M Lyman-α emitting galaxies as tracers. The full VIRUS array is due to be deployed in late 2011 and will provide a powerful new facility instrument for the HET, well suited to the survey niche of the telescope. VIRUS and HET will open up wide field surveys of the emission-line universe for the first time. We present the design, cost, and current status of VIRUS as it enters production, and review performance results from the VIRUS prototype. We also present lessons learned from our experience designing for volume production and look forward to the application of the VIRUS concept on future extremely large telescopes (ELTs).

---

[*] The Hobby – Eberly Telescope is operated by McDonald Observatory on behalf of the University of Texas at Austin, Pennsylvania State University, Stanford University, Ludwig-Maximillians-Universität München, and Georg-August-Universität, Göttingen

[†] G.J.H.: E-mail: hill@astro.as.utexas.edu

[‡] http://hetdex.org/

1. INTRODUCTION: HET WIDE FIELD UPGRADE AND INDUSTRIAL REPLICATION OF VIRUS

Large, targeted, spectroscopic surveys of continuum-selected objects are now becoming the norm, and have greatly increased our understanding in many areas of astronomy. Surveys of the emission-line universe, however, are limited currently to wide field imaging with narrow band filters[1], or to narrower fields with Fabry-Perot etalons or adaptations of imaging spectrographs[2]. Integral field (IF) spectrographs offer a huge gain over these techniques, depending on the application, providing greater sensitivity and wavelength coverage as well as true spectroscopy. The current generation of IF spectrographs is well-adapted to arcminute-scale fields of view, with several thousand spatial elements, and adequate spectral coverage for targeted observations of individual extended objects. They have the grasp to detect simultaneously of order 0.5 million (spectral x spatial) resolution elements.

In order to undertake large-scale surveys for emission-line objects, much greater field coverage is needed. Narrow-band imaging surveys can now cover large areas, but often require spectroscopic follow-up, and still do not probe sufficient volume to detect rare objects or to overcome cosmic variance. Wide-field IF spectroscopy is hard to achieve without a large multiplexing factor, so we have embarked on a program to produce an instrument that uses large-scale replication to create a unique astronomical facility capable of spectroscopic surveys of hundreds of square degrees of sky. The instrument is the Visible Integral-field Replicable Unit Spectrograph (VIRUS)[3-4], a simple, modular integral field spectrograph that is to be replicated at least 150-fold, to provide an order of magnitude increase in grasp over any existing spectrograph, when mounted on the upgraded Hobby-Eberly Telescope (HET)[5,6]. Fig. 1 shows the upgraded HET as it will appear in approximately 18 months from now.
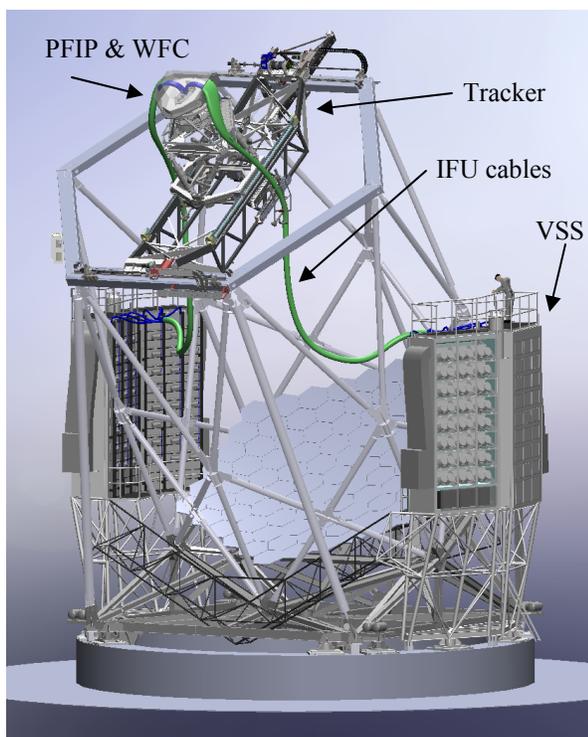

Figure 1 – Upgraded HET as it will appear in late 2011. The new tracker supports the Wide Field Corrector (WFC) and Prime Focus Instrument Package (PFIP). The fiber cables run about 20 m to the four enclosures of the VIRUS Support Structure (VSS) that houses the 75 to 96 pairs of integral field spectrographs that make up VIRUS.

The traditional astronomical instrument has a monolithic design and is a one-off prototype, where a large fraction of the cost is expended on engineering effort. When compared to monolithic instruments, there are cost savings from creating several copies of a spectrograph to gain multiplex advantage, because the components are less expensive and the engineering is amortized over the production run. Several current instruments use small-scale replication to achieve multiplex advantage. These include the DEIMOS[7] and VIMOS[8] imaging spectrographs with two and four copies of each, respectively, within single structures, and the pair of MODS double spectrographs[9] on LBT. The MUSE[10] instrument for ESO VLT will field-slice a 1 arcmin. square field into 24 duplicated spectrographs. VIRUS makes the next step, and exploits industrial-scale replication, which we (arbitrarily) define to be in excess of 100 units. We build upon the concepts laid out in Refs. 1-4, where we concluded that industrial replication offers significant cost-advantages when compared to a traditional monolithic spectrograph, particularly in the cost of the optics and engineering effort. This concept breaks new ground in optical instruments, and appears to be a cost-effective approach to outfitting the coming generation of ELTs, for certain instrument types, where the multiplex advantage can be used to image-slice and thus avoid growth in the scale of instruments with telescope aperture.

The motivation for VIRUS is the Hobby-Eberly Telescope Dark Energy Experiment (HETDEX[11]), which will map the spatial distribution of about 0.8 million Lyα emitting galaxies

(LAEs) with redshifts $1.9 < z < 3.5$ over a 420 sq. deg. area (9 Gpc³) in the north Galactic cap, using VIRUS on the upgraded HET. This dataset will constrain the expansion history of the Universe to 1% and provide significant constraints on the evolution of dark energy. The advantage of an IF spectrograph for this project is that the tracer galaxies are identified and have their redshifts determined in one observation.

Each VIRUS unit is fed by 224 fibers that each cover 1.8 arcsec² on the sky. The fibers feeding a two-unit module are arrayed in a 50×50 arcsec² IFU with a 1/3 fill-factor. A dither pattern of three exposures fills in the area. The spectral resolution is 0.57 nm, with coverage of 350–550 nm. The optical design is simple, using three reflective and two refractive elements. With dielectric reflective coatings optimized for the wavelength range, high throughput is obtained. The full VIRUS array will simultaneously observe a minimum of 33,600 spectra with 12 million resolution elements. The IFUs are arrayed within the 22′ field of the upgraded HET with ~1/7 fill factor, sufficient to detect the required density of LAEs for HETDEX. Development is proceeding with the prototype (VIRUS-P[4]), deployed in October 2006, and the production prototype where value engineering has been used to reduce the cost for production.

The HET[12-15] is the prototype for a new breed of cost-effective large telescopes, and is the basis for the Southern African Large Telescope (SALT)[16]. HET is an innovative telescope with an 11 m hexagonal-shaped spherical mirror made of 91 1-m hexagonal segments that sits at a fixed zenith angle of 35°. It can be moved in azimuth to access about 70% of the sky visible at McDonald Observatory (δ = -10.3° to +71.6°). The pupil is 9.2 m in diameter, and sweeps over the primary mirror as the x-y tracker follows objects for between 50 minutes (in the south at δ = -10.0°) and 2.8 hours (in the north at δ = +67.2°). The maximum time on target per night is 5 hours and occurs at +63°. The HET primary mirror has a radius of curvature of 26164 mm, and the current 4-mirror double-Gregorian type corrector is designed to produce images with FWHM < 0.6 arcsec in the absence of seeing, over a 4 arcmin (50 mm) diameter science field of view. Detailed descriptions of the HET and its commissioning can be found in refs 12-15.

The HET was originally envisioned as a spectroscopic survey telescope, able to efficiently survey objects over wide areas of sky. While the telescope has been very successful at observing large samples of objects such as QSOs spread over the sky with surface densities of around one per 10 sq. degrees, the HET design coupled with the limited field of view of the corrector hampers programs where objects have higher sky densities. In seeking a strong niche for the HET going forward, we desire a wide field of view coupled with a highly multiplexed spectrograph in order to exploit the strengths of the telescope and of the site.

The requirement to survey large areas of sky with VIRUS plus the need to acquire wavefront sensing stars to provide full feedback on the tracker position led us to design a new corrector employing meter-scale mirrors and covering a 22-arcmin diameter field of view. The HET Wide Field Upgrade (WFU) deploys the wide field corrector (WFC[17]), a new tracker prime focus instrument package (PFIP), and new metrology systems[5,6]. The new corrector has improved image quality and a 10 m pupil diameter. The periphery of the field will be used for guiding and wavefront sensing to provide the necessary feedback to keep the telescope correctly aligned. The WFC will give 30 times larger observing area than the current HET corrector. It is a four-mirror design with two concave 1 meter diameter mirrors, one concave 0.9 meter diameter mirror, and one convex 0.23 m diameter mirror. The corrector is designed for feeding optical fibers at f/3.65 to minimize focal ratio degradation, and so the chief ray from all field angles is normal to the focal surface. This is achieved with a concave spherical focal surface centered on the exit pupil. The primary mirror spherical aberration and the off-axis aberrations in the wide field are controllable due to the first two mirrors being near pupils, and the second two mirrors being well separated from pupils. The imaging performance is 0.6 arcsec or better over the entire field of view, and vignetting is minimal (zero within 18 arcmin). The WFC is being manufactured by the University of Arizona College of Optical Sciences.

A new tracker is needed to accommodate the size and five-fold weight increase of the new PFIP. It will be a third generation evolution of the trackers for HET and SALT, and is in essence a precision six-axis stage. The tracker is being developed by the Center for Electro-Mechanics (CEM) at the University of Texas at Austin[18-27], with integration at the CEM facility scheduled for Fall 2010.

HET requires constant monitoring and updating of the position of its components in order to deliver good images. The WFC must be positioned to 10 μm precision in focus and X,Y, and 4.0 arcsec in tip/tilt with respect to the optical axis of the primary mirror. This axis changes constantly as the telescope tracks, following the sidereal motions of the stars. Tilts of the WFC cause comatic images. In addition, the global radius of curvature of the primary mirror can change with temperature (as it is essentially a glass veneer on a steel truss), and needs to be monitored. The segment alignment maintenance system (SAMS) maintains the positions of the 91 mirrors with respect to each other, but is less

sensitive to the global radius of curvature of the surface. The feedback to maintain these alignments requires excellent metrology, which is provided by the following subsystems:

- Guide probes to monitor the position on the sky, and plate scale of the optical system, and monitor the image quality and atmospheric transparency
- Wavefront sensors (WFS) to monitor the focus and tilt of the WFC
- Distance measuring interferometer (DMI) to maintain the physical distance between the WFC and primary mirror
- Tip-tilt sensor (TTS) to monitor the tip/tilt of the WFC with respect to the optical axis of the primary mirror

The upgrade adds wavefront sensing [6,28-31] to HET in order to close the control loop on all axes of the system, in conjunction with the DMI and TTS adapted from the current tracker metrology system. There is redundancy built into the new metrology system in order to obtain the highest reliability. Two guide probes distributed around the periphery of the field of view provide feedback on position, rotation, and plate scale, as well as providing a record of image quality and transparency. The alignment of the corrector is monitored by the wavefront sensors as well as by the DMI and TTS. The radius of curvature of the primary mirror is monitored by the combination of focus position from the WFS with the physical measurement from the DMI and checked by the plate scale measured from the positions of guide stars on the guide probes. The SAMS edge-sensors provide a less sensitive but redundant feedback on radius of curvature as well.

Two guide probes will use small pick-off mirrors and coherent imaging fiber bundles to select guide stars from the outer annulus of the field of view. They will be located ahead of the focal surface, before the shutter. Each will range around the focal surface on precision encoded stages, accessing a 180 degree sector. They are designed to have a small size to reduce shadowing of the focal surface, and each will have a field of view of 22.6 arcsec on a side. During setup on a new target, they will be driven to pre-defined positions, and the initial pointing will be made by centering the guide stars in the probes. This system is a significant upgrade from the current pellicle-based guiders.

Two Shack-Hartmann (S-H) wavefront sensors will also range in the outer field. Their function is to provide feedback on the low-order errors in the wavefront (focus, coma, spherical, and astigmatism)[28-30]. These errors are caused by misalignment of the corrector with the primary mirror focal surface and by global radius of curvature and astigmatism errors in the primary mirror shape. Updates will be generated approximately once per minute. In addition to the WFS probes there will be an analysis wavefront sensor as part of the acquisition camera that will allow more detailed feedback analysis of the image quality, simultaneous with the operation of the WFS probes, independent of seeing. Simulations show that a S-H system with 7x7 sub-apertures across the pupil can meet the requirements using 18th magnitude stars. We have deployed a wavefront sensor for the current HET with 19 sub-apertures across the pupil and the final design is being informed by direct experience with this sensor. The design of the wavefront sensors is straightforward, but their application to the HET, with the varying illumination of the telescope pupil during a track, requires development of a robust software system for analysis of the sensor data to produce reliable wavefront information[30].

2. VIRUS SCIENCE REQUIREMENTS

The design of VIRUS flows directly from the requirements for HETDEX, to maximize the number of LAEs detected in a set observing time, and to span sufficient redshift range to survey the required volume. These science requirements flow down to the following technical requirements for VIRUS:

- Coverage of $\Delta z \sim 2$ and coverage into the ultraviolet to detect LAEs at the lowest possible redshift. VIRUS is designed for $350 < \lambda < 550$ nm or $1.9 < z < 3.5$
- Resolution matching the linewidth of LAEs (R~700) to maximize detectability.
- Minimum throughput on sky (including atmosphere) ranging between 5% at 350 nm, 15% at 450 nm, and 10% at 550 nm to reach sensitivity of $3\text{-}4\times10^{-17}$ erg/cm^2/s in 20 minutes on HET.
- Low read noise detector (~3 electrons) to achieve sky-background dominated observations in 360 seconds
- High stability to ambient temperature variations, though not to gravity variations since the VIRUS modules will be fixed on HET.
- Simple, inexpensive design.

These principles guided the development of VIRUS and the prototype VIRUS-P, as a test-bed for the engineering, and we will discuss the performance of the instrument in light of these requirements in section 3.3.

3. THE VIRUS PROTOTYPE: VIRUS-P

The motivation for building VIRUS-P was to provide an end-to-end test of the concepts behind HETDEX, both instrumental and scientific. It is described in detail in Ref. 4. Construction and testing of VIRUS-P has verified the opto-mechanical design, the throughput, the sensitivity, and demonstrated the utility of such an instrument for surveys of emission-line objects. It has also served as a test-bed for the software development needed for analyzing the data from the full VIRUS array. The parallel nature of VIRUS means that the prototype can be used to develop the final software pipeline. VIRUS-P was also designed to be a facility instrument on the McDonald 2.7 m Smith Reflector. The basic layout is shown in Figure 2. The instrument consists of three basic sub-units: the IFU, the collimator/grating assembly, and the camera assembly. The beam size is 125 mm, allowing the collimator to accept an f/3.32 beam from the fibers, accommodating a small amount of focal ratio degradation of the f/3.65 input from the telescope. In VIRUS-P, the collimator and grating pivot about a horizontal axis passing through the plane of the grating, to allow reconfiguration of the instrument for different wavelength ranges and resolving powers and to shift the blaze of the volume phase holographic grating. Gratings are interchangeable to provide flexibility for different scientific applications. The final VIRUS units will have fixed formats, but will have the capability to swap dispersers. The instrument mounts within a light-tight box that incorporates a lead-screw to adjust the tilt of the collimator with respect to the camera. The camera is a f/1.33 vacuum Schmidt design with a 2k x 2k @ 15 μm pixel CCD at its internal focus.

On the 2.7 m at f/3.65, the 200 μm fiber cores subtend 4.1 arcsec, and the IFU covers 3.5 arcmin^2. While the fibers are large, projected on the sky, the IFU covers the largest area of any current IF spectrograph and this results in great sensitivity for wide area surveys and particularly for spatially extended low surface brightness emission.

VIRUS-P has been designed to mount on the McDonald 2.7 m Smith telescope for testing and to conduct a pilot survey of Ly-α emitting galaxies in support of the HETDEX project. It mounts at the f/9 bent Cassegrain focus, and is fed by a f/3.65 focal reducer (Fig. 2). It is supported within a gimbal in order to mimic the mounting on the HET, where the instrument will be fixed with respect to gravity but will see the full range of operating temperatures. The design is optimized for stability against temperature changes. VIRUS-P has also been mounted on the HET on three occasions to study observing strategy and verify sensitivity limits for the HETDEX survey.
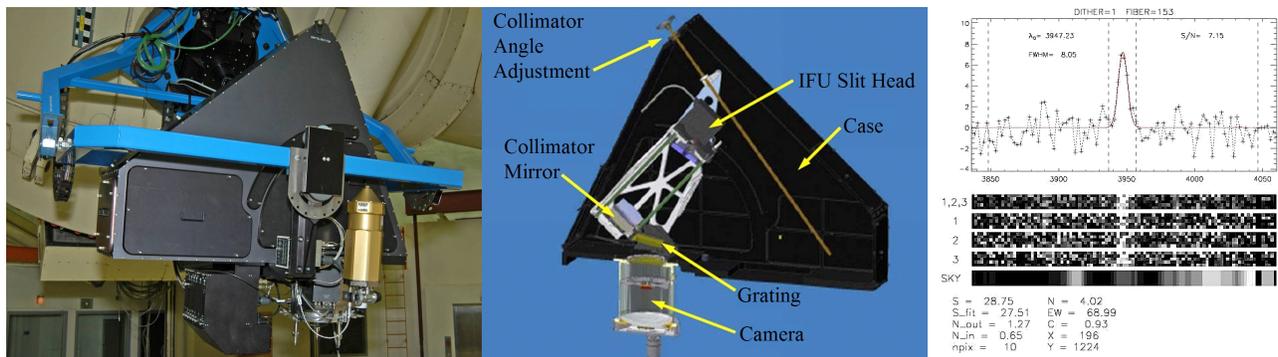

Figure 2. Left shows VIRUS-P installed on the Harlan J. Smith telescope. The blue structure is a gimbal to maintain orientation with respect to gravity. Middle shows the interior components which are fed by an IFU that contains 246 fibers with 200 μm diameter cores. For reference the size of the camera and collimator modules is about 0.6 m. The black case incorporates an adjuster to reconfigure the collimator angle for wavelength range adjustment. A spectrum of a candidate LAE, acquired with VIRUS-P during the pilot survey, is shown on the right. The object is detected in three separate fibers as the IFU position is dithered to fill in the area.

3.1 Integral Field Unit

It is essential to couple VIRUS to the HET with fibers due to the weight and space constraints at the prime focus of the telescope. In addition, the variable effects of the changing pupil illumination of HET during a track are mostly removed by azimuthal scrambling along a fiber, producing much greater stability in the data calibration than is possible with an imaging spectrograph. Fiber IFUs can utilize microlens arrays, providing close to 100% fill-factor[32], or be of the simpler "densepak" type[33]. For VIRUS we have elected to use the densepak type of bare fiber bundle to maximize throughput and minimize cost[34]. The primary advantage of lenslets is in coupling the slower f/ratios of typical foci to

the fast ratio required to minimize focal ratio degradation[35], and such IFUs are ideal for retro-fitting existing spectrographs. Lenslets do not provide perfect images, however, so if there is flexibility to choose the input f/ratio to the fibers and if the fill-factor can be tolerated, trading it against total area, the bare bundle provides the best efficiency[2]. We use a fill factor of 1/3, with the fibers in a hexagonal close pack, and dither the IFU arrays through three positions to fill the area. Note that if the f/ratio of the microlens case is the same as the f/ratio from the telescope in the bare-fiber case, and the lenslets subtend the same area on the sky as the bare fibers, then the fill-factor of the densepak type array is exactly offset by the larger area that the bundle covers per exposure. So in the case where maximum areal coverage is required, the bare bundle is the preferred solution[2].

Development of the prototype IFUs at the Astrophysikalisches Institut Potsdam (AIP)[34] and University of Texas at Austin (UT)[36] has explored ways of setting up the required matrix of fibers at the input end. Setting up a matrix of fused silica capillary tubes to set the spacing proved very successful, but time-consuming to set up. The alternative, adopted for production, is to use micro-drilled alloy blocks to locate the fibers at the input. Anti-reflection coated fused silica cover plates are bonded (immersed) to the polished surface of each IFU with index-matching couplant to minimize insertion losses. Measurements of FRD and throughput before and after immersing the ends demonstrate marked improvement for many fibers, and results in very uniform throughput between fibers [36]. At the output of the bundle, the fibers are arrayed in a line, immersed against the curved back face of a cylindrical lens, and fanned out with their axes pointing perpendicular to the collimator mirror (and to the lens). This layout allows collimation of the beam to be achieved with only one spherical mirror, leading to a very efficient design. The spacing between fibers is achieved by bonding the fibers to a monolithic groove plate of stainless steel. Figure 3 shows images of the slit and input ends of fiber cables produced during development.
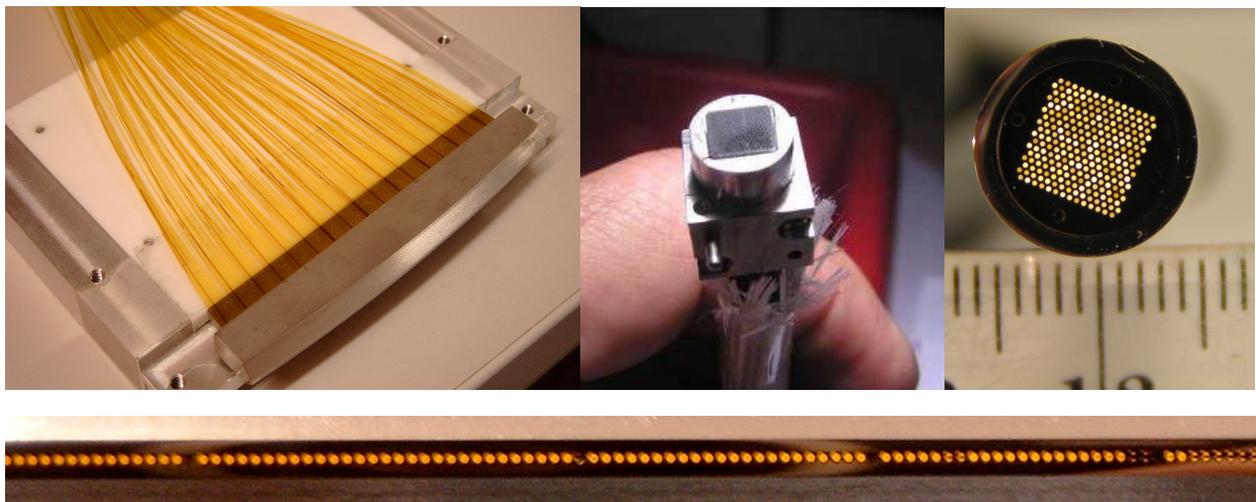

Figure 3: IFU development. Left shows pseudo-slit output of the IFU bundle. The fibers are arrayed on a precision grooved plate that sets the spacing and angle between fibers. The fibers are arrayed perpendicular to the back surface of a cylindrical lens bonded to the convex surface of the plate. Middle and Right show input heads with the matrix set by fused silica capillaries and drilled block, respectively. Bottom shows a section of the output slit. The pitch of the fibers is 320 μm, resulting in a separation of 7.8 pixels on the CCD.

3.2 Optomechanical Design

While the VIRUS units are mounted in fixed housings, their enclosures track ambient temperature and they are required to operate with high stability under a wide range of temperature from -5 to +25 degrees Celsius. The instrument is specified to not require recalibrating for shifts in the positions of the fiber spectra over the temperature range encountered in an hour, with the goal of maintaining alignment during an entire night. Stability is crucial since the data analysis is sensitive to 0.1 pixel shifts in the spectra. This requirement corresponds to shifts smaller than 0.5 pixels (1/10 of a resolution element) at the detector for 5 degrees Celsius temperature change. VIRUS-P was designed to test this requirement. It is mounted in a gimbal to maintain its orientation, but sees the full temperature swing in a night. In

addition, we designed the prototype to test all possible modes of the instrument, including a range of resolving powers and wavelengths, even if these will not be options for the majority of VIRUS units, in practice.

The optical and mechanical design of VIRUS-P is discussed in Refs 4,37-39. The instrument has a collimator and disperser module and a catadioptric camera with a cryogenic detector head at its internal focus. The majority of the collimator parts are of aluminum with Invar metering rods maintaining the spacing between the collimator mirror and the IFU output. In the collimator, three Invar rods act as rails to which the optics are mounted, with simple adjustments and clamps. The rods are bolted at one end to the IFU reference plate of aluminum (to which the IFU slit head mounts), and at the other to disk flexures mounted in an aluminum plate. A similar metering structure inside the camera maintains focus and alignment. This setup effectively allows the structure to have the CTE of aluminum in all dimensions except the optical axis where Invar is needed to maintain focus. Tests show that the instrument is extremely stable, so this design has proven successful.

Design of the VIRUS-P camera is covered in detail in Ref. 38. The camera is an evacuated Schmidt design, with the detector at the internal focus. It has f/1.33 for the nominal pupil size of 115 mm, and accepts light from a 125 mm diameter pupil with little vignetting. The optics consist of the fused silica window which has an aspheric front surface (maximum deviation 0.3 mm), the spherical mirror, and the fused silica field flattener with a spherical front and aspheric back surface. The detector and field flattener are suspended in the beam, causing approximately 23% areal obstruction, on axis. The excellent FRD performance of the fibers results in the preservation of the central obstruction from the telescope and hence reduces the effect of the detector obstruction to some extent. Otherwise the design has very high efficiency, and produces superb images. High quality images are required to maintain sufficient separation between the spectra from individual fibers on the detector, allowing clean extraction of the spectra and maximizing the number of fibers per spectrograph.

The CCD has 2k x 2k format with 15 μm pixels. Working into the near-UV, low readout noise and good UV-blue QE are important considerations. VIRUS-P uses a back-side illuminated Fairchild 3041 detector. Read noise with this system is measured as 4.2 electrons at 100 kpxl/s and 3.6 electrons at 25 kpxl/s [38].

The camera mechanical design follows the same principles as the collimator, using aluminum for the housing and Invar metering rods to maintain the focus of the camera mirror with respect to the detector. Flexures between the mirror assembly and the housing provide the radial constraint. The detector and field flattener are suspended in the beam with a stainless spider assembly that also carries the cold link and flex circuit. The design has been optimized for minimum obstruction. Flexures incorporated into the spider design decouple the expansion of the aluminum housing from the detector head position[38]. The field flattener is mounted to the spider with clips at each corner. The CCD package is clamped to the cold block with clips, and a frame of Ultem 1000 polyetherimide provides thermal isolation from the rest of the spider assembly.

Volume phase holographic (VPH) gratings offer high efficiency and low cost. The standard setup originally envisioned for HETDEX employs a volume phase holographic (VPH) grating with 831 fringes per mm, and Bragg angle close to 11 degrees. The clear aperture of the grating is 130 mm. We have undertaken tests of small and full size gratings from Wasatch Photonics and Kaiser Optical Systems International (KOSI), using a custom automated test-bench that can fully characterize a grating over a range of input and output angles[39]. This test bench will be used to evaluate the gratings for the full VIRUS array. Performance in the ultraviolet has been enhanced by reducing the angle of incidence to shift the blaze to the UV. Angle changes of the grating at fixed collimator angle have little effect on the wavelength range, so tilting the grating provides an independent free parameter in tuning the throughput as a function of wavelength. This is equivalent to tilting the fringes in the grating, but allows standard setups and processing for untilted fringes to be employed, reducing cost. The ability to independently tilt the angle of the collimator and grating in VIRUS-P has allowed the instrument to be set up for optimal performance for the grating, as measured in the lab. Subsequently we have added higher resolution gratings covering the blue, green, and red, up to 680 nm, which offer resolving powers between 2500 and 4000.

3.3 Performance

VIRUS-P has been in service since October 2006. It has been used primarily on the McDonald 2.7 m Smith Reflector for a pilot survey to study the properties of Lyman-α emitting (LAE) galaxies[40]. Figure 2 shows an example LAE detected in this survey. On three occasions we have taken the instrument to the HET for a series of tests of its

performance to confirm predicted sensitivities. Detailed discussion of the performance of VIRUS-P is presented in Ref. 4, here we summarize the results:

- Throughput of VIRUS-P as a function of wavelength (ignoring aperture effects at the input to the fibers) peaks at 40% with 15 m long fibers, in line with predictions based on the measured throughputs of individual components. On-sky, including the atmosphere, the throughput peaks at 18%. This performance meets or exceeds that required for HETDEX, except at the very shortest wavelengths.

- The 5-σ point source line flux sensitivity is ~5×10^{-17} erg/cm^2/s, in 2 hours observing, in line with predictions. Significant numbers of emission-line galaxies are being detected.

- Image quality of the instrument meets requirements. Optical alignment was achieved with simple setup procedures.

- The instrument is extremely stable against temperature changes, with images moving 1/20 of a resolution element with a 12 Celsius temperature change, exceeding requirements. On HET, the VIRUS units will be mounted fixed, so stability against gravity vector changes is not a requirement.

VIRUS-P is being used for an extensive survey of the properties of LAE galaxies, in order to better understand their evolution and large-scale clustering in preparation for HETDEX. The survey covers 166.4 arcmin^2 on the COSMOS, MUNICS-S2, and GOODS-N fields and detects 107 LAEs and 368 low redshift emitters[40]. This survey is providing confirmation that we can detect LAEs in the expected numbers and discriminate them from low redshift galaxies. Other science applications have included high redshift radio galaxies[41], and studies of resolved nearby galaxies[42,43].

4. VIRUS PRODUCTION DESIGN

Evolution of the design of VIRUS from the prototype to the production model was made in two steps. First a pre-production prototype was developed that incorporates the production engineering to reduce costs. In particular aluminum castings for major substructures and the cryostat were prototyped and qualified. Second, small design modifications gleaned from this experience have been incorporated and we will enter production with an initial batch of 10 units, in early 2011, followed by full production. Assembly and testing of the VIRUS modules will take place at Texas A&M University, where a large lab complex has been allocated to the project.
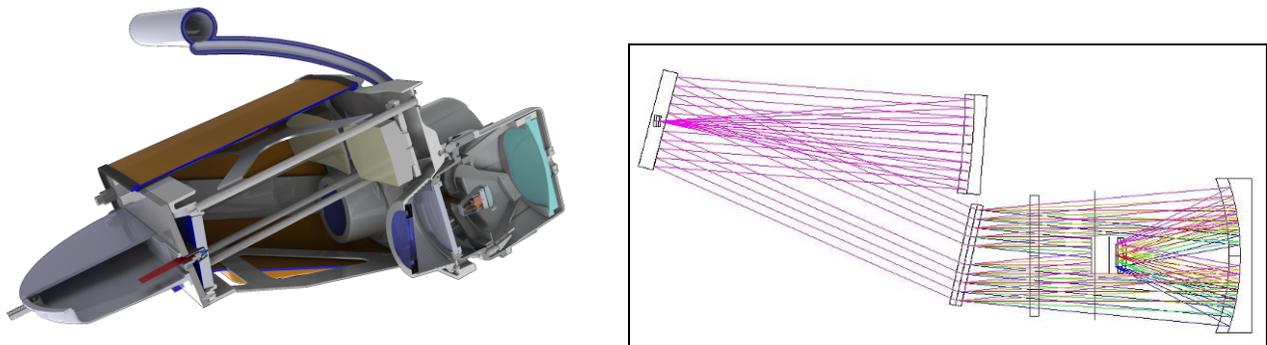

Figure 4: Layout of the production VIRUS. Left shows the production mechanical design and right shows the optical design with the grating and camera rotated 180 degrees about the optical axis to make the design more compact. The grating has 930 l/mm and the coverage is fixed at 350-550 nm. The mechanical cutaway shows the IFU slit assembly on the left, mounted to the collimator. The Schmidt camera has an internal CCD in the vacuum and mounts to the main bulkhead of the collimator. It is cooled by a flexible line from above with a breakable cryogenic bayonet connection.

4.1 VIRUS Production Optomechanical Design

We have made some significant changes to the design, based on experience with VIRUS-P and responding to the development for the HET WFU design. The most significant is to double the spectrographs so that a pair shares a single IFU, a common collimator housing, and a common cryostat (Fig. 4). The motivation for this came first from fiber cable handling: it is more efficient in terms of weight and cross-sectional area to double the number of fibers in a cable (note that the fiber itself is not the dominant weight in a bundle). There is not a significant cost-savings on the IFU, since the

majority of the cost is in the fiber, but volume occupied by the cables is reduced and the cable handling becomes significantly easier with 75 instead of 150 cables to accommodate (the goal is 92 cables, and the IFU handling system is being designed for this number). The other advantage to the double unit is that two cameras share a vacuum, and have a single connection to the LN_2 cooling system. This increases the volume in an individual cryostat, which increase hold-time, and saves cost on vacuum valves and other fixturing. Pairing the spectrographs enabled reduction of mechanical structure to support optics by eliminating the redundant structure of two spectrographs placed side-by-side. The complexity of the superstructure to house the 150+ spectrographs could also be reduced by pairing the instruments because fewer interfacial features between instrument and superstructure are required.

The optical layout has been modified to make the system more linear and allow the units to be packed more tightly in the housings (Fig. 4). Analysis of the fiber diameter for maximizing the number of Lyman-α emitting (LAE) galaxies detected by the HETDEX survey indicates that the ideal is 1.5 arcsec for the expected range of image quality to be encountered in the survey (1.3 to 1.8 arcsec FWHM). Analysis of the expected number of LAEs with redshift also indicates that the majority of the objects are located at z<3.5 due to the change in distance modulus with redshift coupled with the steepness of the LAE luminosity function. As a result, the decision has been made to reduce the wavelength coverage so as to preserve spectral resolution, while accommodating the larger fibers (266 vs 200 μm core diameter). This is a small change and the increase in dispersion of the grating (930 versus 830 l/mm) does not effect diffraction efficiency over the observed bandpass. Wavelength coverage is 350 – 550 nm (1.9 < z < 3.5) and resolving power is R=700 at 450 nm. Fig. 5 shows an exploded view of the spectrograph unit.

The VIRUS optics and mechanical interfaces have been carefully specified to produce optics that will be interchangeable amongst any VIRUS unit. Both the optical and mechanical properties of each optic have been carefully toleranced using Monte Carlo realizations of the collimator and camera that were then combined and evaluated. The optical tolerancing is described in detail in Ref 44. Particular attention has been paid to the relative alignment of the axes of the two spectrographs within a single unit. This analysis indicates that any camera can be used with any collimator, and will enable quick assembly of the optical assemblies and spectrograph units. The aim is to make the optical alignment process of the subassemblies and the complete instrument more straightforward and rapid (see section 4.4, below).

Detailed information on the VIRUS mechanical design including the extensive use of castings is given in Ref 45. Relatively early in the production mechanical design of VIRUS we investigated castings for large aluminum bulkhead parts. Castings offer the ability to produce part shapes which would otherwise be impossible or prohibitively expensive to machine from a solid billet of material. As a result they offer the designer structures that are exceedingly lightweight and stiff. Casting is often characterized by its lack of precision and repeatability which does not lend itself well to producing instrumentation. In addition, casting processes traditionally require high up-front costs for fabricating the molds making them uneconomical for low-quantity production and risky for design efforts where prototyping is required. We have adapted our design to these factors, and the recent proliferation of stereo lithography and other rapid prototyping devices has significantly decreased the cost of producing prototype castings. Complex part shapes are quickly and economically "printed" using stereo lithography equipment or machined from plastic foam. Those parts can then be used to imprint sand molds or in the case of investment casting, coated with refractory material and melted out through a sprue. Several companies offer fast turnaround, low cost prototype casting services and can accept CAD models online without need for mechanical drawings. As a result, we were able to prototype subassemblies with castings without incurring prohibitive costs, and were able to gain an understanding of the design principles needed in using castings.
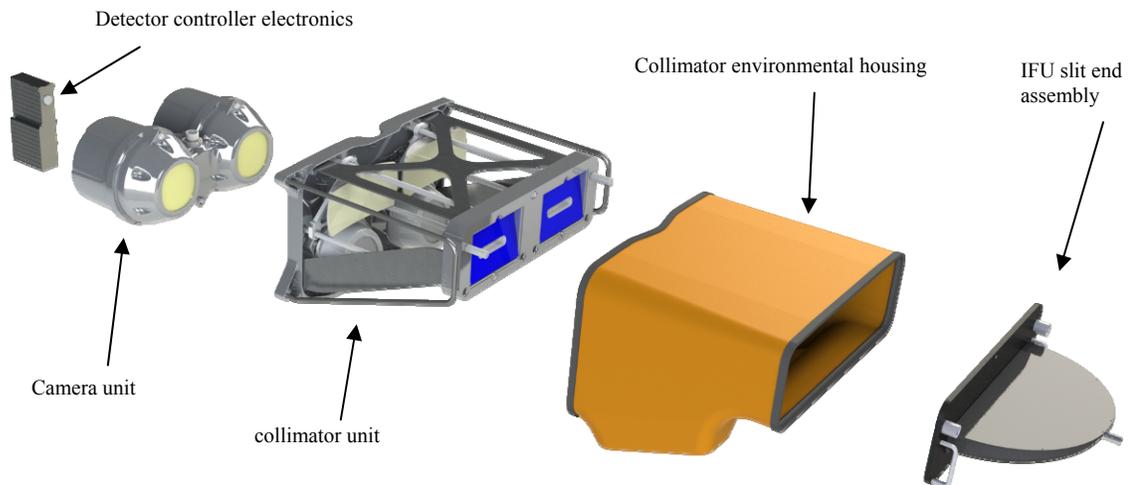
Figure 5. Basic components of the VIRUS unit housing two spectrographs. Light enters at the IFU slit assembly along two axes. The collimator holds the IFU and camera cryostat on kinematic mounts and forms the main structure of the instrument. The cameras are interchangeable and removable should maintenance be required. The detector controllers mount directly to the cryostats.

Kinematic mounts enable highly repeatable registration between components and their use is prevalent in precision optical assemblies. The VIRUS spectrograph relies on kinematic mounts between sub-assemblies which are considered modular to each other, specifically the IFU slit assembly, the collimator, and the camera. The optical and mechanical tolerances of the instrument are arranged such that modules of a particular type would be interchangeable. For example, the camera couples to the collimator through a kinematic mount. It is required that any camera could be used with any collimator and perform within specification. Similarly, the VPH gratings are modular to the collimator and the detector sub-assemblies are modular to the camera body.

The kinematic mounting features also serve as reference datums during fabrication. This is a key design adaptation that allows a low precision casting to be used in a high precision assembly with the minimum of post-machining. In VIRUS we use three ball-in-vees to create the kinematic mounts between the IFU slit and camera subassemblies that interface at the two large cast plates in the collimator structure. The raw cast parts are first machined for the kinematic features on their outer faces, and these then form the kinematic mount for the rest of the machining of the optical mount features, which is done in a single setup on the inside of the part. In this way, the amount of machining is minimized and the optics are referenced as directly as possible to the kinematic mount points that tie the whole assembly together.

The camera cryostat vacuum is also shared between a pair of spectrographs. This modification effectively halves the number of ancillary vacuum components such as valves and vacuum gauges. This saves not only the expense of these components but reduces the number of sealing surfaces which contribute to long-term vacuum degradation and are a point of failure. The larger evacuated volume also leads to longer vacuum hold-time. Similarly, the cryogenic cooling system is shared within a unit. This reduces the part count of the instrument cryogenic system and also simplifies the cryogenic distribution system and losses associated with fittings and valves. The cryogenic system development and testing is described in greater detail in Sec. 5.1 and Ref. 46. The cryostat is composed of two aluminum castings, post-machined on critical mount surfaces and flanges. Five prototypes have been delivered by MKS Inc., and have been evaluated extensively. An impregnating step with Locktite Resinol, following machining ensures that the porosity of the cast aluminum does not lead to virtual leaks or poor vacuum seals, and leak rates are achieved that are consistent with the O-ring length and internal volume of the cryostat. While the tooling cost for casting is quite significant, the cost for even a single cryostat of this size is competitive with machining from bulk stock, and much cheaper for even small-batch production runs like those we have already undertaken.

The stability of the instrument to temperature changes is crucial, as discussed above. While the VIRUS-P design was very successful in this regard, we have traced the small instability with ambient temperature swings to movement of the camera mirror. In VIRUS the detector head assembly is all Invar with a cast "spider" mounting the detector and field flattener and an Invar truss structure supporting the mirror.

4.2 Integral field unit cables

The HET site has a median seeing of 1.0 arcsec FWHM, and we initially adopted 1 arcsec^2 per fiber (200 μm core diameter) on the upgraded HET for maximum sensitivity. Subsequent analysis of the trade-off between areal coverage and sensitivity indicates that larger fibers are preferred for HETDEX to maximize the number of detected LAE galaxies. As a result, 1.5 arcsec (266 μm) diameter is the requirement for the production VIRUS units. The current HET corrector is f/4.65, but the future wide-field corrector will have f/3.65. The optics of VIRUS can accommodate an f/ratio of f/3.32 (within the 125 mm pupil size), allowing some focal ratio degradation and accommodation of alignment errors in the subsystems. IFU development at AIP and UT has focused on establishing a design that minimizes FRD, maximizes throughput, and is manufacturable in quantity[34].

The fiber cables each contain 448 fibers and we have kept the design as simple and lightweight as possible (Fig 6). The input head consists of a precision micro-drilled block into which the fibers are fed which is in turn clamped within a stainless steel shell that provides the mounting features. The fibers are glued in with epoxy and then cut off and polished. At the exit, the cable bifurcates within a slit housing into two slits with the fibers glued to grooved blocks of the same design as for VIRUS-P (See Sec. 3.1). Input and output are bonded to a thin fused silica plate and a cylindrical lens, respectively, both AR coated.

The physical design of the cables has benefitted greatly from the use of prototype bundles on VIRUS-P, which has been taking data for 3 years. We uncovered an interesting behavior when fibers in the corners of the square input array started to show variable and lower throughput on the sky. This was traced to the way the cable was being handled. This cable was 15 m long to allow VIRUS-P to be deployed on the HET and each month it was coiled and uncoiled during the mounting process. Twists introduced into the cable resulted in a torsional force at the head, which affected the fibers in the corners, preferentially. This was verified with tests in the lab which revealed significant stress-induced FRD for these fibers. Shaking out the cable relieved the stress and we now dress the cable in a large loop rather than coiling it up. Interestingly the effect did not show itself until after more than a year of use, so it is possible that the constant handling of the cable caused these fibers to become more sensitive to the torsional stress. In this respect the long track-record of VIRUS-P has proven valuable in evaluating the design. We plan an extensive lifetime test of a fiber cable where we manipulate it through the motions expected for a decade of use on HET in about a month, while looking for signs of FRD. The design of the test is described in Ref. 47, along with a description of the fiber cable routing on the telescope.

Figure 6. Production IFU cables at AIP. Left and middle images show the slit assembly with the two slit blocks that feed the pair of spectrographs within a VIRUS unit. The slit assembly mounts to the collimator kinematically. The cable length is 22 m. Right shows nine IFUs input heads mounted as they will be at the HET focus. Three screws and a pin locate the heads. AR coated cover plates are not yet applied in this view. The heads have a ¼ fill-factor in the field of view. This configuration provides the ability to fill in the field of view by offsetting the telescope to four positions.

The conduit housing the fiber cables has undergone an extensive design evaluation and prototyping. It is important that the fiber not piston significantly in and out of the conduit where it exits the cable into the slit box. Such pistoning might occur with changes in axial load or ambient temperature swings, and we are particularly concerned about shipping and handling during installation. We also wish to minimize the weight of the conduit which can dominate the total weight, and have adopted a custom fully interlocked aluminum conduit with PVC sheathing supplied by Hagitec. The ID is 13 mm. As with our previous cables we have an inner sock of Kevlar to protect the fiber from the internal structure of the conduit. In order to stabilize the length of the conduit we tension this inner sock at assembly so that the

conduit is somewhat compressed and the resultant spring constant is high. The Kevlar sock has a minimum diameter chosen so as not to constrict the fiber, but still fit in the ID of the conduit. We have taken this design through the full range of motions expected at HET (and more) and not seen any sign of the fiber pistoning in and out of the conduit at its exit. The first nine cables have been delivered to AIP and are undergoing testing. Full production will start in late 2010.

The exit focal ratio from the cable and the position of the pupil from each fiber at the instrument pupil depend on more than FRD. Tilts of the fibers (individually and as a group) at the input make the exit focal ratio faster, and tilts at the slit cause the pupil to translate in the instrument. The VIRUS optical design allows for 10 mm extra pupil diameter, and all these effects have been toleranced and added to the FRD, so that in total at least 95% of the light passes unvignetted through the instrument pupil.

4.3 Detector System and Alignment of Camera

The CCDs for VIRUS have 2kx2k format with 15 μm pixels. The required readout time is relatively slow at 20 seconds, binned 2x1, but low read noise (~3 electrons) is required and the parallel readout of up to 192 CCDs (~400 Mpxl) is still challenging. The data volume from the full VIRUS array (of up to 192 spectrographs) is about 2.5 GB per observation. Observation times per field are 20 minutes for the HETDEX survey, and we expect to generate 40 TB of raw data over the course of the survey, including calibrations. These data volumes are quite modest in the context of the coming generation of large imaging surveys. The data reduction pipeline will reduce each night's data in 8 hours, requiring around 128 processors at today's speeds.

In writing the specifications for the detector system, we developed metrics applied to batches of CCDs to obtain the required final science performance on average. This approach is important in keeping costs low because restrictive requirements reduce yield and increase risk and price. A good example of how we approached this is the metric for QE and read noise which is based on S/N ratio for the expected signal level from the sky for VIRUS observations. The metric will be calculated for the average of a batch of detectors, along with a minimum QE threshold as a function of wavelength and a maximum read noise threshold for any CCD. This allows the vendor to balance poorer read noise with increased QE and vice versa and provides greater latitude for accepting CCDs without impacting the performance we care about. The resultant increased yield provides the vendor with greater security of predicting yields and hence provide the best price.

The other key specifications are very low cross-talk between the pair of CCDs in each cryostat, and between cryostats, and very low external noise pickup. Since we are searching for detections which are very few correlated resolution elements, we need to understand the noise characteristics of the data extremely well.

The integrated detector system will be provided by Astronomical Research Cameras, Inc., with the University of Arizona Imaging Technology Laboratory providing thinned backside illuminated CCDs with AR coatings optimized for the VIRUS bandpass, as a subcontract from wafers manufactured by Semiconductor Technology Associates, Inc. Since the CCDs come from a custom wafer run, we have elected to increase the imaging area to 2064 by 2064 pixels, allowing more latitude for alignment.

The design of the detector package, flex circuit, and controller have been highly customized to the VIRUS application, since the engineering is spread over a large production run. This allowed us to remove most of the complexity associated with the detector head of VIRUS-P. Figure 7 shows the layout for a pair of detectors in a single cryostat. The package, machined from Invar-36, is designed for minimum obstruction and hides in the shadow of the field flattener (FF) lens. The CCDs will be flat to within +/-10 μm which is allowed by the tolerance analysis. The package has a custom header board that brings the traces to a single connector on one side of the package. A custom flex circuit with complex geometry connects the two detectors to a single 55-pin hermetic bulkhead connector (Fig. 7). The controller connects directly to this connector, without cables, and its form-factor has been customized to fit between the cylinders of the cryostat cover.

The detector package also mounts the FF lens on four Invar flexure clips that set the separation and alignment of the FF to the detector plane. Metrology of each detector will be used to control these dimensions when the clips are glued to the field flattener, with the glue-line acting to take up any misalignment. The alignment jig incorporates a laser to establish the axis of the detector head and allows the field flattener to be aligned using the interference pattern generated by its front and back surfaces. Tests show this scheme has 10 μm sensitivity to tilts and decenter within the required

tolerance. Once the FF lens is installed its optical axis defines the axis of the head and allows alignment within the camera.
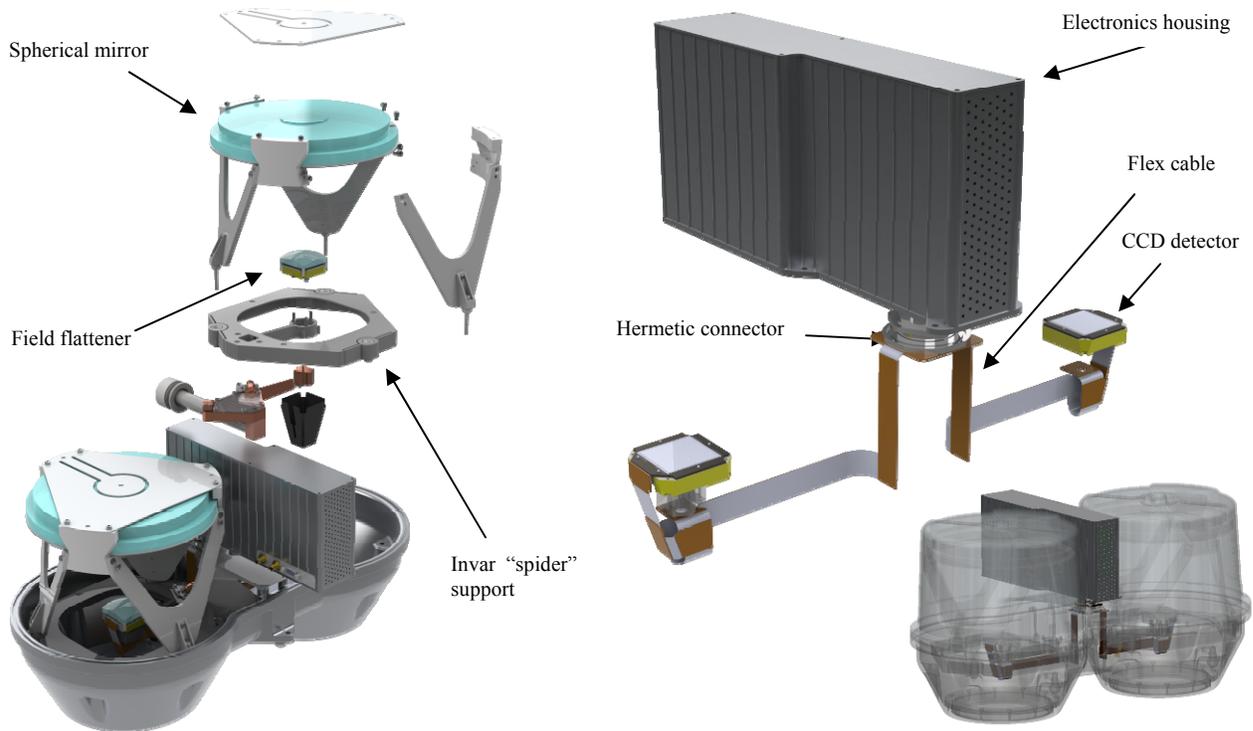

Figure 7. Camera assembly and electronics. Left shows the integration of the two camera channels into the cryostat. Right shows the detector system controller, the flex circuit, and the CCD packages as they integrate into the cryostat.

The detector package with attached FF is then integrated into the "spider" which supports the detector head, cantilevered in the beam. The spider is of post-machined cast Invar-36, and its production is discussed further in Ref. 45. The whole spider is adjusted in all degrees of freedom in an alignment jig to position the FF on the axis of a laser that defines the camera axis. Four lugs are then glued in place to capture the alignment, and they interface to machined features in the cryostat housing. In this way, the alignment of the CCD and FF to the axis of the camera can be achieved within the required tolerances of 50 μm in centration and separation, and 0.05 degrees in tilt[44]. Prototypes of these jigs will be tested on the first pair of detectors due to be delivered in August 2010.

Final alignment of the camera will be made against a fiducial collimator, grating, and IFU positioning the camera mirror for best focus over the field. This will be done with the detector cold and will utilize a special cryostat back with feed-throughs to make the adjustments and clamp the mirror. The IFU will be pistoned through focus to map out the focal surface versus the plane of the CCD to make the adjustment as deterministic (and hence as quick) as possible. The cryogenic system is described in Section 5.1.

The shutter for the system is located in front of the IFU inputs, just below the focal surface in the PFIP. It has a rotary blade design, and a minimum exposure time of 1 second. The shutter is located remotely from the detector controllers and is commanded separately. Exposures are coordinated via the Telescope Control System, which sends simultaneous shutter-open commands to the shutter control system and to the VIRUS Data Acquisition System (VDAS) that controls the detector system. Timing between the shutter and the VDAS is maintained with a Network Time Protocol server, synchronized to GPS time.

The CCD controllers have DC power in and fiber-optic data lines out. To minimize crosstalk, the timing of all CCD clocks is synchronized to a master clock signal distributed over a Low-Voltage Differential Signal (LVDS) system. The data system requires several levels of multiplexing. First, each CCD controller commands two detectors, each with

possibly two readout amplifiers. Next, a custom-built 8-way multiplexer combines the output from each set of 8 CCD controllers. Next, the output of each of 12 multplexers is fed into a PCI interface card. Two PCI-to-PCIe expansion chassis are used to connect 6 PCI interface cards each to a PCIe port in the VDAS computer. Finally, the data are transferred via DMA from the PCI interface cards into the VDAS memory. From there, the data are passed to a "QuickLook" pipeline, and also written to disk as 192 separate FITS files, one for each detector, to aid parallel processing of the pixels in an on-site array of CPUs. The QuickLook pipeline includes many of the algorithms developed for the full reduction of the VIRUS dataset, but is focused on monitoring detector health and data quality, to inform the observer of problems, and when to terminate observations due to poor conditions.

4.4 Assembly and test plan

The assembly and test of VIRUS will take place at Texas A&M University (TAMU), where a production line is being set up[48,49]. A large newly outfitted lab space is being adapted to the production line. The assembly flow is being detailed down to the part level in preparation for assembling the first units in August 2010, and lessons learned from that exercise will be incorporated into the production assembly starting in early 2011.

We have spent considerable design time thinking about how to assemble the unit spectrographs in the most straightforward way. In particular, we have made an effort to minimize difficult and complicated assembly tasks, time-consuming operations, and procedures that require more than one person to complete. While the total number of parts is not generally a large cost or assembly time driver in an average astronomical instrument, it certainly is a consideration in the manufacture and assembly of VIRUS. With this factor in mind we have made efforts to minimize the total number of manufactured parts that compose the instrument. One way this is accomplished is through the use of several cast aluminum parts as detailed above.

The design allows us to precisely pre-align the optics in subassemblies which are then mounted to the instrument structure. In this way, the only adjustment within the collimator is to align the spherical mirror, and similarly in the camera as described above. It is a design requirement that the camera units be interchangeable amongst any collimator unit once the instrument is mounted on the telescope. This requirement will enable "hot-swapping" of cameras during operations and minimize down time of the instrument in the case of failures, vacuum pump downs, etc. In order to meet this requirement we plan to align each VIRUS collimator with a "fiducial" camera and align each camera with a "fiducial" collimator. These fiducial units will be mechanically and optically identical to the other VIRUS units, and will provide a constant reference for the optical alignment amongst all 150+ VIRUS spectrographs. In this way, careful alignment of the fiducial subassemblies will then allow a minimum of extra jigs to be used in the subsequent alignment of the manufactured units.

A key interface is between the IFU slit assembly and the collimator. These components will be assembled in different locations (AIP and TAMU) and must be properly aligned to a common pair of optical axes. This will be achieved with an aluminum jig plate that defines the two optical axes within a unit. The plate has two precision flats with reticles mounted such that the centration and separation of the axes is captured and the normal to each flat defines the axis vector. Two jig plates will be produced and used in each location to set up the alignment jigs for the subassemblies.

5. DEPLOYMENT ON HET

5.1 Cryogenic system

The distributed layout of the VIRUS array presents a significant challenge for the cryogenic design[50,46]. Allowing 5 W heat load for each detector, with all losses accounted for and a 50% margin, the cooling source is required to deliver 3,600W of cooling power. We engaged Applied Cryogenics Technology to evaluate the options and provide an initial design. Following a trade off between cryocoolers, small pulse-tubes and liquid nitrogen based systems, it is clear that from a reliability and cost point of view liquid nitrogen is the best choice[51]. The problem of distributing the coolant to the distributed suite of spectrographs is overcome with a gravity siphon system fed by a large external dewar. A trade-off between in-situ generation of the LN_2 in an on-site liquefaction plant, and delivery by tanker has been made, with the result that the delivery option is both cheaper and more reliable. The 11,000 gallon holding dewar would have in excess of 4 weeks operation capacity, and would be refilled every 2 weeks. The cryogenic system is illustrated in Fig. 8.

An important aspect of the cryogenic design is the requirement to be able to remove a camera cryostat from the system for service, without impacting the other units. This is particularly difficult in a liquid distribution system. A design has been developed that combines a standard flexible stainless steel vacuum jacketed line (SuperFlex) to a cryogenic bayonet incorporating copper thermal connector contacts into each side of the bayonet. When the bayonet halves are brought together they close the thermal contact. The resulting system is completely closed, i.e., it is externally dry with no liquid nitrogen exposure. The camera end of the connector is connected by a copper cold finger to the detector. This design has another desirable feature: in normal operation the SuperFlex tube slopes downwards and the bayonet is oriented vertically. Liquid evaporation will flow monotonically up in order to avoid a vapor lock. If the bayonet is unscrewed and raised upwards, a vapor lock will occur and the bayonet will be cut off from the cooling capacity of the liquid nitrogen. This effectively acts as a "gravity switch", which passively turns off cooling to that camera position.

We have made extensive tests on prototypes, applying heat loads to the bayonet, which have performed very well[46]. The temperature rise across the connection is $\Delta T \sim 1.8$ K/Watt of load at 80 K. Modeling of the full thermal path has been undertaken, under the requirement of having the CCD temperature at -140 C, with no heater power. The performance of the bayonet is significantly better than the requirement, and represents less than 20 K temperature rise across the connection for the expected load. We will run the CCDs at a temperature between -100 and -110 C, controlled via heating resistors and a control loop based on an RTD sensor. The performance of the bayonet is not changed when the connection is broken and remade. We are now building a lab setup to simultaneously cool six VIRUS units, which will be used during the production assembly, and testing of the cameras.
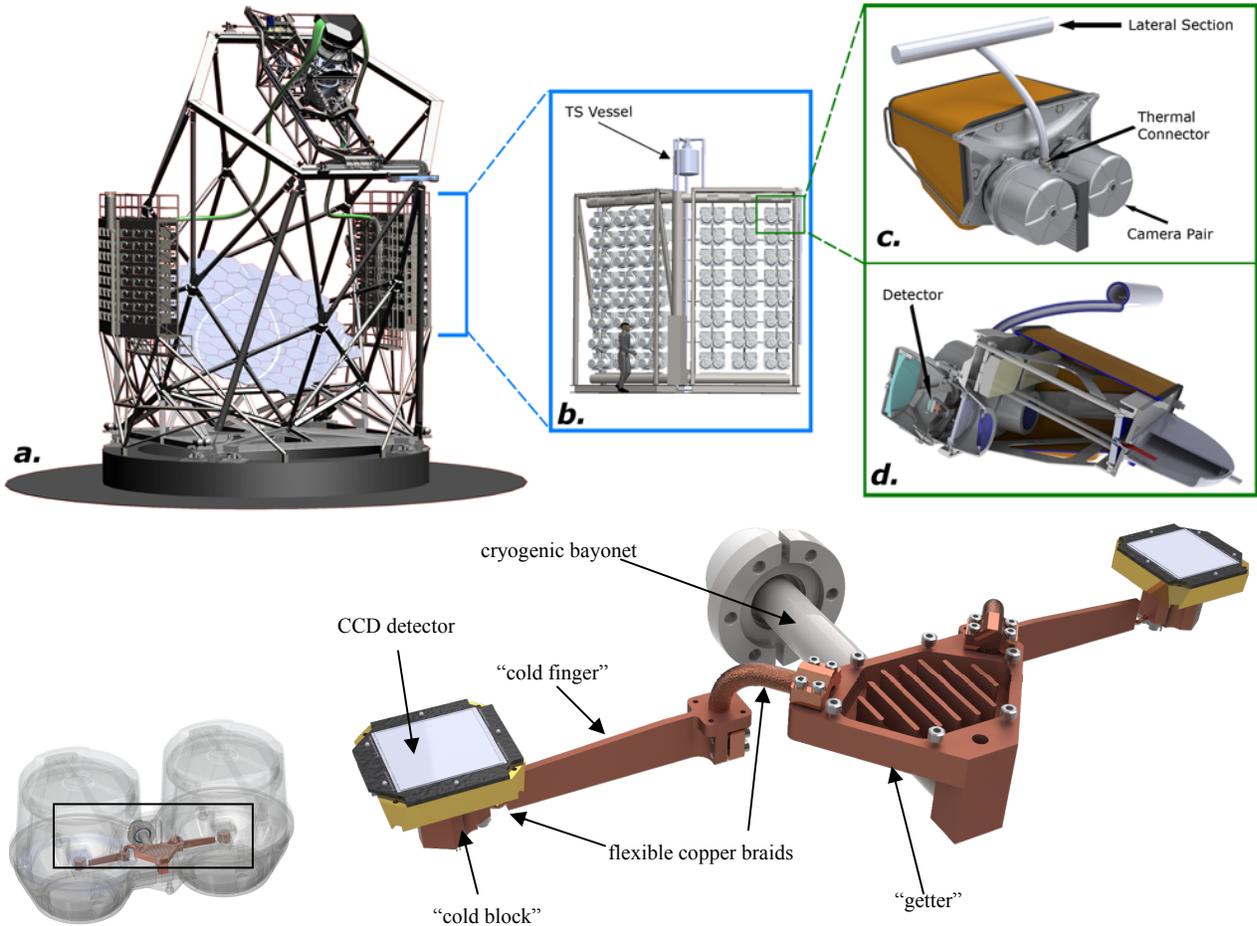

Figure 8. Camera cryogenic system. Top panels show the liquid nitrogen distribution system on the telescope and thermal connector to the cryostat. An external dewar keeps the two thermal siphon (TS) vessels filled, which feed the manifolds. The lower panels show the cold link interior to the cryostat which cools two detectors via cold links from the bayonet.

5.2 VIRUS Support Structure, IFU Cable Handling, and VIRUS Maintenence

The science drivers for VIRUS require high throughput at $\lambda > 350$ nm. This argues for minimizing the length of fiber in the integral field units. Initially, locations around the top hexagon of the HET structure were explored, resulting in a minimum fiber length of 15 m. Models linking instrument performance to sensitivity and predicted number of LAEs detected in the HETDEX survey allowed a trade-off between fiber length, cost, and survey requirements. Analysis of the structure required to support the VIRUS instruments (total weight 30,000 kg) indicated that there is significant expense associated with the high location, and we have undertaken a trade-off between performance and location of VIRUS, with the result that we have chosen a lower location for the VIRUS enclosures with a 20 m average length of IFU fiber[15,51].

The VIRUS support structure (VSS[52]), shown in Fig. 1, supports and houses the spectrograph units and rotates on air bearings with the telescope structure when the azimuth is changed. The four enclosures can each house up to 24 VIRUS units. They have access panels for each unit to allow servicing of an individual unit, and circulate filtered, conditioned air that is controlled in temperature to track the ambient temperature sufficiently well that the surface of the enclosures is within 0.5 C of ambient. It is a goal to use part of the cooling capacity of the boil-off from the liquid nitrogen system to remove heat generated by the detector controllers, since the gaseous nitrogen must be exhausted exterior to the telescope at close to ambient temperature so as not to pollute the thermal environment of the telescope.

VIRUS is designed for low maintenance with no moving parts. The camera vacuum and detector controllers will be the items that will require maintenance. As a result we have developed the cryogenic bayonet[50,46] described in Sec. 5.1 to allow the cameras to be removed without breaking into the liquid nitrogen cooling system. The bayonets allow an individual camera to be warmed up for vacuum maintenance or removed for more extensive work. We project that the vacuum will remain within operational bounds for at least 6 months without needing ion pumps, based on experience with similar systems and direct measurements of O-ring leak rates on the production prototype cryostats. A rotating schedule of pumping down a column of 8 units every 2 weeks is expected to keep the cryostats operating with a minimum of personnel time. In the event of a problem, the detector controllers can be swapped easily and then diagnosed for problems off the telescope. Experience and guidance from the vendor indicate that component failures in the controllers will be rare but are likely to be the most common problem. Controllers can be tested off the cryostats and swapped rapidly if needed. Further diagnosis will be at the level of board swaps, with spares provided by the vendor.

6. DESIGN FOR REPLICATION LESSONS LEARNED

6.1 Optomechanical Design for Minimum Cost

Designing an instrument for production has proven to have significant differences from normal "one-off" astronomical instruments where there is a trade between time spent on design and analysis and time spent in assembly and test. The amortization of significant non-recurring engineering effort over many copies, coupled with the multiplier penalty for time-consuming assembly and test activities, shifts the emphasis onto extensive design analysis, prototyping and pre-qualification of subassemblies and jigs, before production starts. This was expected, but the degree to which up-front effort reduces cost is quite striking. Production start-up can be quite lengthy but subsequent assembly-line production can then go very quickly. Time spent understanding and developing the production process is essential.

The other key lesson is that the optical design should be sufficiently within the state of the art that it is possible to create pre-aligned subassemblies that bolt together using CNC machine-level tolerances (20-100 μm, depending on the machine). The individual optics should have sizes that are manufacturable at many companies to ensure competition. For spherical mirrors the limit is around 300 mm. The design can make use of aspheric optics, and they now can provide a very cost-effective solution, minimizing the number of elements, if the tolerances of CNC grinding-polishing machines and profilometry can be tolerated. This is the case with the VIRUS design, and such elements can be made inexpensively to about 250 mm diameter. Tighter tolerances depend mainly on metrology, and in sufficient volume interferometric tests with computer generated holograms become cost-effective.

The fabrication of large numbers of identical instruments creates an opportunity for cost savings inherent to purchases in bulk. Just as the price of off-the-shelf items is reduced for purchases of large quantity, the price of custom fabricated parts are typically lower when ordered in large quantities. This is often due to savings through ammortization of non-recurring engineering charges such as fixturing and to end-loading which is the natural improvement in speed a

technician gains through repetition. The proliferation of computer controlled machines in optical production is having an effect on costs for production quantities, even if they are used only for initial shaping.

Care should be taken not to over-specify tolerances on optics and mechanical parts. Tight tolerances have only minor effects on project cost for one-off instruments, but can drive costs significantly in quantity. Evaluation of performance in the metric of S/N ratio rather than absolute image quality, for example, can lead to relaxation of critical tolerances. Understanding that manufactured components will exhibit a range of quality and incorporating that into Monte-Carlo modeling of performance also allows specification of requirements by batch which can allow a risk reduction for the manufacturer and a commensurate lowering of the cost. These principles were applied to the detector system and optics of VIRUS and have resulted in significant cost savings.

Our experience is that once quantities reach 100 much of the cost-benefit from mass-production has been realised. This is particularly the case for optics which are considerably more expensive per unit for quantity 50. In sufficient quantities the optics cost about ¼ of the single-unit price.

6.2 Software Development

One place where the parallelized nature of VIRUS is a huge advantage is in data reduction software development. Many instruments have suffered from the late arrival of reduction software or from unexpected instrumental features that require the development of new software methods to account for them. Since the VIRUS units will be very close to identical, and very similar to VIRUS-P, we have had the advantage of having a full test-bed for the software in operation for several years.

The software for VIRUS must process a highly parallel data stream, quickly, and detect single-line objects, reliably. Development of the final software pipeline for reduction of VIRUS data is being led by MPE. Since VIRUS is naturally a parallel instrument, all the requirements for and attributes of the software have been developed and tested on the prototype. This was a key motivation for the deployment of VIRUS-P on the telescope early in the project. Two pipelines have been developed, one in Texas called VACCINE[40] and the other in Munich, called CURE. VACCINE has been used primarily to reduce and analyze data from the pilot survey on the McDonald 2.7 m, while the algorithms of CURE are tuned for use on the HET. The difference is driven primarily by the plate scale difference between the telescopes. On the 2.7 m, the fibers are significantly larger than the image size, while on HET they are comparable. This leads to differences in the detection algorithm, but not the data reduction methods. Care is being taken to propagate errors and avoid interpolation through resampling of data, which leads to position-dependent smoothing and can alter the noise characteristics. CURE uses a Bayesian detection algorithm that assigns a likelihood of a source to every (spatial and spectral) resolution element. Tests show robust rejection of cosmic rays and reliable detection of 5-σ line flux objects, as required for HETDEX. The stability requirements for the instrument (Sec. 3) are driven by the need to know the statistical weight of each pixel, particularly in the spatial dimension, across the fiber profiles, where small movement of the image on the detector can change the weights greatly. We have also demonstrated sky subtraction to the Poisson noise limit, with both pipelines, aided by the fact that most of the fibers of VIRUS are observing sky in any exposure.

We have exploited the advantage to having the ability to exercise software on real data this early in the project, and we expect to come on line with a fully operational and debugged pipeline when VIRUS is turned on, not least because early production VIRUS units will be used on sky prior to deployment of the full instrument. This is a key advantage of a highly replicated instrument, particularly since such instruments by definition generate large volumes of data.

7. THE VIRUS FUTURE

VIRUS was designed from the outset to allow exchange of gratings to change wavelength ranges and resolutions, and VIRUS-P is used on the McDonald 2.7 m Smith Telescope with four different VPH gratings. Due to the large size of the fibers projected on the sky, it is very sensitive for low surface brightness extended features, for which the sensitivity surpasses that of instruments on the largest telescopes. In addition to this flexibility and sensitivity, the generic nature and massively replicable characteristic of the instrument can allow us to adapt the instrument to a wide range of not only telescope diameters (1m ~ 40m), but also observing modes (single to multiple objects), in a very cost-effective manner. On small telescopes, the IFU can cover very large fields of view with large spatial elements ideal for studying resolved galaxies, while on large telescopes the same IFU can observe single objects in varying image quality, while

obtaining a simultaneous background observation. VIRUS allows many different slicing modes between field and wavelength coverage/resolution, and a few of them are illustrated in the following examples.

7.1 Adaptation of VIRUS for other science applications

The current HET Low-Resolution Spectrograph[52] is incompatible with the WFU and will be replaced with a more capable broad-band fiber-fed instrument based on VIRUS, called LRS2[53]. It takes advantage of the fact that VIRUS was designed to be easily adapted to a wide range of spectral resolutions, and wavelength ranges by changing dispersers and optics coatings. LRS2 is fed by a 7x12 arcsec^2 lenslet coupled fiber IFU, covers 350-1100 nm, simultaneously at a fixed resolving power R~1800, with the wavelength range split with dichroics into four channels shared between two VIRUS units, one for the blue and red wavelength range (350 - 630 nm) and the other for the red and far-red range (630-1100 nm). It uses the multiplex power of VIRUS to cover wavelength, rather than wide area. Only minimal modification from the base VIRUS design in gratings (for both units) and in the detectors (to fully depleted thick CCDs for the far-red unit only) is required. We expect to deploy the blue unit when we install VIRUS. LRS2 is a powerful instrument serving the HET strengths in survey follow-up, synoptic observations, and transient events. It will be particularly useful for following up emission-line objects detected with VIRUS at higher resolution, and can be used in parallel with VIRUS.

The other immediate evolution of the VIRUS design has been the instrument VIRUS-W, destined for the new Munich Wendelstein Observatory[54]. The instrument is targeted at studies of resolved galaxies, specifically spiral galaxy bulges, a proven strength of VIRUS-P. It uses many of the design elements of VIRUS, but aims for higher resolution over a more restricted bandpass. The camera is refractive and two VPHG grisms can be exchanged to observe 475 - 560 nm at R~2300 or 493 - 544 nm at R~6500. The IFU has 267 fibers, each 4.24 arcsec diameter covering a field of 144 x 75 arcsec^2.

7.2 VIRUS on future ELTs and Other Telescopes

It is interesting to consider deployment of a VIRUS unit on a future ELT. In this context, it should be noted that the product of image quality to pupil size for the upgraded HET (~1.3 arcsec on a 10 m) is comparable to proposed ELTs (site seeing 0.4 arcsec and ~30 m pupils) even for natural seeing. Hence we can expect similar performance for a VIRUS deployed on GMT, TMT, or EELT, without the cost associated with scaling up the pupil size of more traditional spectrographs with telescope aperture– we might even consider VIRUS the first ELT instrument!

VIRUS can be deployed as a more conventional fiber-fed multi-object spectrograph, though we feel that small IFUs are much preferred to single fibers since variations in seeing and object size will be covered. Taking 7-fiber deployable mini-IFUs on a 30 m class telescope, each VIRUS unit could observe 70 objects with each IFU covering 1.0 arcsec diameter with 170 micron fibers. Even with half the IFUs assigned to sky measurement to allow for beamswitching between IFUs, each VIRUS unit will cover 35 objects. The wavelength coverage could be modified by exchanging dispersers, up to R~3000 with the current design. IFUs also provide some spatial resolution and the ability to perform reliable spectrophotometry without slit losses. These mini-IFUs would be an ideal application for hexabundles[55]. Full wavelength coverage of 350-1100 nm at R~1800, analogous to LRS2, would be achievable with suitable input optics and VIRUS is perhaps the optimal instrument to combine with the adaptive focal plane concept pioneered by the AAO[56]. We are considering these concepts for a future instrument on GMT, and an instrument along these lines is being evaluated for VLT[57].

As a rough cost guide for such an instrument, VIRUS places a fiber on sky for ~$500 cost, in production or $8k/object in the above example with beamswitching, plus the cost of a fiber positioning system. Comparable imaging spectrograph designs with slitlets have very large optical elements and present significant challenges for the opto-mechanical design. They also cost a factor of 2-3 more than a comparable VIRUS-based spectrograph with the same total grasp (number of objects observed multiplied by the number of spectral resolution elements). There are small throughput penalties in using fibers, but the prospect of spectroscopic observations of a thousand of objects on an ELT for a spectrograph cost of under $5M is certainly attractive. We estimate a full system with LRS2-type spectrographs and a $10M positioner would cost around $25M and would be capable of observing 1000 objects over 350-1100 nm, simultaneously.

On a smaller scale, VIRUS-P has demonstrated the power of using a 10-m class IF spectrograph on a 2-m class telescope for resolved galaxy dynamical, stellar population, and star formation studies[42,43]. VIRUS-P has revitalized the McDonald 2.7 m Smith reflector and resulted in heavy over-subscription during dark time. The cost of a single VIRUS

unit is within reach of many smaller observatories. IF spectrographs are adaptable to any telescope aperture and the availability in VIRUS of what can be characterized as a "commodity" spectrograph promises to deliver a great boon to small telescopes as well as future ELTs.

8. SUMMARY AND STATUS

HETDEX, consisting of the WFU, VIRUS, and the blind spectroscopic survey of 420 sq. degrees is 80% funded and procurement of all major components for the WFU and VIRUS is underway. The tracker will be assembled and tested at CEM at the end of 2010, allowing six months for characterization and software development. In parallel, the production of VIRUS will start at the end of 2010 with the first delivery of detectors. We are planning for deployment of the upgrade and VIRUS in about 12 months from the time of writing. In the meantime the VIRUS-P prototype has been taking data for 3 years and the design is being adapted into new instruments with a wide range of capabilities.

ACKNOWLEDGEMENTS

REFERENCES

1. e.g. M. Ouchi, M., et al., "Large-Scale Filamentary Structure around the Protocluster at Redshift z = 3.1," ApJ, **634**, 125 (2005); Gronwall, et al., "Lyα Emission-Line Galaxies at z = 3.1 in the Extended Chandra Deep Field-South," ApJ, **667**, 79 (2007); L. Guaita, et al., "Ly-α Emitting Galaxies at z = 2.1 in ECDF-S: Building Blocks of Typical Present-day Galaxies?" ApJ, **714**, 255 (2009);
2. e.g. C. Martin et al., "A Magellan IMACS Spectroscopic Search for Lyα-emitting Galaxies at Redshift 5.7," ApJ, **679**, 942 (2008); M. Rauch et al., "A Population of Faint Extended Line Emitters and the Host Galaxies of Optically Thick QSO Absorption Systems," ApJ, **681**, 586, (2008)
3. G.J. Hill, P.J. MacQueen, P. Palunas, A. Kelz, M.M. Roth, K. Gebhardt, & F. Grupp, "VIRUS: a hugely replicated integral field spectrograph for HETDEX", *New Astronomy Reviews*, **50**, 378 (2006); G.J. Hill, P.J. MacQueen, J.R. Tufts, A. Kelz, M.M. Roth, W. Altmann, P. Segura, M. Smith, K. Gebhardt, & P. Palunas, "VIRUS: a massively-replicated IFU spectrograph for HET," *Proc. SPIE*, **6269**-93 (2006)
4. G.J. Hill, P.J. MacQueen, M.P. Smith, J.R. Tufts, M.M. Roth, A. Kelz, J. J. Adams, N. Drory, S.I. Barnes, G.A. Blanc, J.D. Murphy, K. Gebhardt, W. Altmann, G.L. Wesley, P.R. Segura, J.M. Good, J.A. Booth, S.-M. Bauer, J.A. Goertz, R.D. Edmonston, C.P. Wilkinson, "Design, construction, and performance of VIRUS-P: the prototype of a highly replicated integral-field spectrograph for HET", *Proc. SPIE*, **7014**-257 (2008)
5. R.D. Savage, J.A. Booth, K. Gebhardt, J.M. Good, G.J. Hill, P.J. MacQueen, M.D. Rafal, M.P. Smith, B.L. Vattiat, "Current Status of the Hobby-Eberly Telescope Wide Field Upgrade and VIRUS", *Proc. SPIE*, **7012**-10 (2008)
6. R. Savage, et al., "Current Status of the Hobby-Eberly Telescope wide field upgrade," Proc. SPIE, **7733**-149 (2010)
7. S. Faber *et al*., "The DEIMOS spectrograph for the Keck II Telescope: integration and testing," Proc. SPIE, **4841**, 1657 (2003)
8. O. Le Fevre *et al*., "VIMOS and NIRMOS multi-object spectrographs for the ESO VLT," Proc. SPIE, **4008**, 546 (2000)

9. R.W. Pogge et al., "The multi-object double spectrographs for the Large Binocular Telescope", Proc. SPIE, 7735-9 (2010)

10. R.M. Bacon "The second-generation VLT instrument MUSE ", Proc. SPIE, **7735**-7 (2010)

11. Hill, G.J., Gebhardt, K., Komatsu, E., Drory, N., MacQueen, P.J., Adams, J.A., Blanc, G.A., Koehler, R., Rafal, Roth, M.M., Kelz, A., Grupp, F., Murphy, J., Palunas, P., Gronwall, C., Ciardullo, R., Bender, R., Hopp, U., and Schneider, D.P., 2008, "The Hobby-Eberly Telescope Dark Energy Experiment (HETDEX): Description and Early Pilot Survey Results", in Panoramic Views of the Universe, ASP Conf. Series, vol **399**, p 115 (arXiv:0806.0183v1)

12. J.A. Booth, M.J. Wolf, J.R. Fowler, M.T. Adams, J.M. Good, P.W. Kelton, E.S. Barker, P. Palunas, F.N. Bash, L.W. Ramsey, G.J. Hill, P.J. MacQueen, M.E. Cornell, & E.L. Robinson, "The Hobby-Eberly Telescope Completion Project", in *Large Ground-Based Telescopes*, Proc SPIE **4837**, 919 (2003)

13. J.A. Booth, P.J. MacQueen, J.G. Good, G.L. Wesley, P.R. Segura, P. Palunas, G.J. Hill, R.E. Calder, "The Wide Field Upgrade for the Hobby-Eberly Telescope", Proc. SPIE, **6267**-97 (2006)

14. G.J. Hill, P.J. MacQueen, M.D. Shetrone, & J.A. Booth, "Present and future instrumentation for the Hobby-Eberly Telescope", Proc. SPIE, **6269**-5 (2006)

15. G.J. Hill, P.J. MacQueen, P. Palunas, S.I. Barnes, M.D. Shetrone "Present and future instrumentation for the Hobby-Eberly Telescope", Proc. SPIE, **7014**-5 (2008)

16. D.A.H. Buckley, G.P. Swart, J.G. Meiring, "Completion of the Southern African Large Telescope", *Proc. SPIE*, **6267**-19 (2006)

17. J. H. Burge, S. D. Benjamin, M. B. Dubin, S. M. Manuel, M. J. Novak, Chang Jin Oh, M. J. Valente, C. Zhao, J. A. Booth, J. M. Good, G. J. Hill, H. Lee, P. J. MacQueen, M. D. Rafal, R. D. Savage, M. P. Smith, B. L. Vattiat, "Development of a wide-field spherical aberration corrector for the Hobby Eberly Telescope", Proc. SPIE, **7733**-51 (2010)

18. J. Good, et al., "Design of performance verification testing for HET wide-field upgrade tracker in the laboratory," Proc. SPIE, **7739**-152 (2010)

19. M.S. Worthington, et al., "Design and analysis of the Hobby-Eberly Telescope Wide Field Upgrade bridge," Proc. SPIE, **7733**-147 (2010)

20. N.T. Mollison, et al., "Design and development of a long-travel positioning actuator and tandem constant force actuator safety system for the Hobby-Eberly Telescope wide field upgrade," Proc. SPIE, **7733**-150 (2010)

21. G.A. Wedeking, et al., "Kinematic optimization of upgrade to the Hobby-Eberly Telescope through novel use of commercially available three-dimensional CAD package," Proc. SPIE, **7733**-148 (2010)

22. J.J. Zierer, et al., "The development of high-precision hexapod actuators for the Hobby-Eberly Telescope dark energy experiment (HETDEX)," Proc. SPIE, **7733**-49 (2010)

23. J.R. Mock, et al., "Tracker controls development and control architecture for the Hobby-Eberly Telescope Wide Field Upgrade," Proc. SPIE, **7733**-152 (2010)

24. B.J. South, et al., "Wind loading analysis and strategy for deflection reduction on the HET Dark Energy Experiment upgrade," Proc. SPIE, **7733**-51 (2010)

25. M.S. Worthington, et al., "Design and development of a high-precision, high-payload telescope dual-drive system," Proc. SPIE, **7733**-201 (2010)

26. N.T. Mollison, et al., "Collaborative engineering and design management for the Hobby-Eberly Telescope wide field upgrade," Proc. SPIE, **7738**-84 (2010)

27. J. H. Beno, J.A. Booth, J. R. Mock, "An alternative architecture and control strategy for hexapod positioning systems to simplify structural design and improve accuracy ", Proc. SPIE, **7733**-97 (2010)

28. H. Lee, et al., "Analysis of active alignment control of the Hobby-Eberly Telescope wide field corrector using Shack-Hartmann wavefront sensors," Proc. SPIE, **7738**-18 (2010)

29. H. Lee, et al., "Metrology systems for the active alignment control of the Hobby-Eberly Telescope wide-field upgrade," Proc. SPIE, **7739**-28 (2010)

30. H. Lee, et al., "Orthonormal aberration polynominals over arbitrarily obscured pupil geometries for wavefront sensing in the Hobby-Eberly Telescope," Proc. SPIE, **7738**-59 (2010)

31. H. Lee, et al., "Surface figure measurement of the Hobby-Eberly Telescope primary mirror segments via phase retrieval and its implications for the wavefront sensing in the new wide-field upgrade," Proc. SPIE, 7738-58 (2010)

32. e.g. J.R. Allington-Smith *et. al*., "Integral Field Spectroscopy with the Gemini Multiobject Spectrograph. I. Design, Construction, and Testing", PASP, **114**, 892 (2002)

33. S.C. Barden & M.A. Wade, "DensePak and spectral imaging with fiber optics", in *Fiber optics in astronomy*; Proceedings of the Conference, Tucson, AZ, Apr. 11-14, 1988 (A90-20901 07-35). San Francisco, CA, Astronomical Society of the Pacific, 1988, p. 113-124

34. A. Kelz, S.M. Bauer, F. Grupp, G.J. Hill, E. Popow, P. Palunas, M.M. Roth, P.J. MacQueen, U. Tripphahn, "Prototype development of the integral-field unit for VIRUS", *Proc. SPIE*, **6273**, 121 (2006)

35. e.g. J. Schmoll, M.M. Roth, & U. Laux, "Statistical Test of Optical Fibers for Use in PMAS, the Potsdam Multi-Aperture Spectrophotometer," PASP, **115**, 854 (2003)

36. J.D. Murphy, P. Palunas, F. Grupp, P.J. McQueen, G.J. Hill, A. Kelz, M.M. Roth, "Focal ratio degradation and transmission in VIRUS-P optical fibers", *Proc. SPIE*, **7018**-104 (2008)

37. M.P. Smith, G.J. Hill, P.J. MacQueen, W. Altman, J.A. Goertz, J.M. Good, P.R. Segura, G.L. Wesley, "Mechanical design of VIRUS-P for the McDonald 2.7m Harland J Smith Telescope", Proc. SPIE, **7014**-259 (2008)

38. J.R. Tufts, P.J. McQueen, M.P. Smith, P.R. Segura, G.J. Hill, R.D. Edmonston, "VIRUS-P: camera design and performance", *Proc. SPIE*, **7021**-10 (2008)

39. J.J. Adams, G.J. Hill, and P.J. MacQueen, "Volume Phase Holographic Grating Performance on the VIRUS-P Instrument", *Proc. SPIE*, **7014**-258 (2008)

40. J.J. Adams, et al, "HETDEX Pilot Survey – I. Survey design, performance, and catalog", ApJ, in prep., (2010)

41. J.J. Adams, G.J. Hill, and P.J. MacQueen, "B20902+34: a collapsing proto-giant elliptical galaxy at z=3.4", ApJ, **694**, 314 (2009)

42. G.A. Blanc, A. Heiderman, K. Gebhardt, N.J. Evans, J. Adams, "The Spatially Resolved Star Formation Law From Integral Field Spectroscopy: VIRUS-P Observations of NGC 5194", ApJ, **704**, 842 (2009); G.A. Blanc, et al., "The VIRUS-P Exploration of Nearby Galaxies (VENGA): Survey Design and First Results", in *Third Biennial Frank N. Bash Symposium, New Horizons in Astronomy*, ASP Conf. Ser., in press (2010) (2010arXiv1001.5035B)

43. P. Yoachim et al.,, ApJ, 716, L4-8 (2010).

44. H. Lee, et al., "VIRUS optical tolerance and production," Proc. SPIE, **7735**-140 (2010)

45. B. Vattiat, et al., "Mechanical design evolution of the VIRUS instrument for volume production and deployment," Proc. SPIE, **7735**-264 (2010)

46. T.S. Chonis, et al., "Development of a cryogenic system for the VIRUS array of 150 spectrographs for the Hobby-Eberly Telescope," Proc. SPIE, **7735**-265 (2010)

47. I. Soukup, et al., "Design of the fiber optic support system and fiber bundle accelerated life test for VIRUS," Proc. SPIE, **7735**-180 (2010)

48. J.L. Marshall, et al., "Production-line assembly of 150+ VIRUS spectrographs," Proc. SPIE, **7735**-163 (2010)

49. A. Collins, et al., "Development of VIRUS alignment assembly fixtures," Proc. SPIE, **7735**-263 (2010)

50. M.P. Smith, G.T. Mulholland, J.A. Booth, J.M. Good, G.J. Hill, P.J. MacQueen, M.D. Rafal, R.D. Savage, B.L. Vattiat, "The cryogenic system for the VIRUS array of spectrographs on the Hobby Eberly Telescope", *Proc. SPIE*, **7018**-117 (2008)

51. J.T. Heisler, et al., "Integration of VIRUS spectrographs for the HET dark energy experiment," Proc. SPIE, **7733**-153 (2010)

52. Hill, G. J., Nicklas, H., MacQueen, P. J., Tejada de V., C., Cobos D., F. J., and Mitsch, W., "The Hobby-Eberly Telescope Low Resolution Spectrograph", in *Optical Astronomical Instrumentation*, S. D'Odorico, Ed., Proc. SPIE, **3355**, 375 (1998)

53. H. Lee, et al., "LRS2: a new low-resolution spectrograph for the Hobby-Eberly Telescope and its application to scalable spectrographs for the future of extremely large telescopes," Proc. SPIE, **7735**-276 (2010)

54. M.H. Fabricius, S. Barnes, R. Bender, N. Drory, F. Grupp, G.J Hill, U. Hopp, P.J. MacQueen, "VIRUS-W: an integral field unit spectrograph dedicated to the study of spiral galaxy bulges", *Proc. SPIE*, **7014**, 234 (2008)

55. J. Bland-Hawthorn, et al., "Hexabundles: imaging fibre arrays for low-light astronomical applications", Proc. SPIE, **7735**-144 (2010)

56. e.g. W. Saunders, et al., "MANIFEST: a many instrument fiber positioning system for GMT ", Proc. SPIE, **7735**-230 (2010)

57. A. Kelz, et al., "ERASMUS-F: pathfinder for an E-ELT 3D instrumentation ", Proc. SPIE, **7739**-96 (2010)